Metaplasticity mechanisms restore plasticity and associativity in an animal model of Alzheimer's disease

Qin Li[a,1], Sheeja Navakkode[b,c,1], Martin Rothkegel[a], Tuck Wah Soong[b,c], Sreedharan Sajikumar[a,b,c,2,3], and Martin Korte[a,d,2,3]

[a]Division of Cellular Neurobiology, Zoological Institute, Technische Universität Braunschweig, D-38106 Braunschweig, Germany; [b]Department of Physiology, Yong Loo Lin School of Medicine, National University of Singapore, 117597 Singapore; [c]Neurobiology/Ageing Programme, National University of Singapore, 117456 Singapore; and [d]Helmholtz Centre for Infection Research, Arbeitsgruppe Neuroinflammation und Neurodegeneration, 38124 Braunschweig, Germany

Dynamic regulation of plasticity thresholds in a neuronal population is critical for the formation of long-term plasticity and memory and is achieved by mechanisms such as metaplasticity. Metaplasticity tunes the synapses to undergo changes that are necessary prerequisites for memory storage under physiological and pathological conditions. Here we discovered that, in amyloid precursor protein (APP)/presenilin-1 (PS1) mice (age 3–4 mo), a prominent mouse model of Alzheimer's disease (AD), late long-term potentiation (LTP; L-LTP) and its associative plasticity mechanisms such as synaptic tagging and capture (STC) were impaired already in presymptomatic mice. Interestingly, late long-term depression (LTD; L-LTD) was not compromised, but the positive associative interaction of LTP and LTD, cross-capture, was altered in these mice. Metaplastic activation of ryanodine receptors (RyRs) in these neurons reestablished L-LTP and STC. We propose that RyR-mediated metaplastic mechanisms can be considered as a possible therapeutic target for countering synaptic impairments in the neuronal networks during the early progression of AD.

metaplasticity | hippocampus | synaptic tagging | APP/PS1 mice | L-LTP

Alzheimer's disease (AD), the most frequent form of dementia, is an age-related neurodegenerative disorder clinically characterized by early declarative memory deficits, followed by deterioration of other cognitive functions (1). The memory loss in AD is characterized by extracellular accumulation of amyloid β protein (Aβ) in the hippocampus and cerebral cortex preceding neurodegeneration (2, 3). Increasing evidence suggests that soluble forms of Aβ interfere with hippocampal synaptic plasticity mechanisms known to mediate learning and memory processes, including long-term potentiation (LTP) and long-term depression (LTD) of excitatory synaptic transmission (4–8). In particular, the protein synthesis-dependent late phase of LTP (L-LTP) is impaired in the hippocampus of various AD transgenic mouse models and in Aβ-treated hippocampal slices (4, 9), whereas LTD is facilitated (10) or not altered (10–12). It has been reported recently that Aβ-induced inhibition of LTP is mediated by extrasynaptic NMDA receptor activity, which prevents phosphorylation of the transcription factor cAMP response element-binding protein (13, 14).

Synaptic plasticity can be governed by a previous activity of the same postsynaptic neuron or neural network, a phenomenon referred to as metaplasticity (15). Metaplasticity orchestrates multiple aspects of functional plasticity and thus promotes long-term memory storage (16). For instance, inducing metaplasticity by activating ryanodine (RYA) receptors (RyRs) with its agonist RYA in hippocampal CA3–CA1 synapses lowers the threshold of LTP, resulting in enhanced LTP induction and persistence (17, 18). In addition, metaplasticity can influence processes of associative memory storage as in the case for synaptic tagging and capture (STC) (17). STC is defined as the associative interactions between two independent sets of synapses within the same neuronal network, in which a synaptic "tag" set by a transient activity captures plasticity-related proteins (PRPs) generated from a nearby strong

event, leading to late plasticity (19, 20). Metaplasticity can extend the duration of the synaptic tag, thus ensuring late associativity for a prolonged period during STC (17).

In the present study, we conducted experiments on a well-established AD transgenic mouse model [amyloid precursor protein (APP)/presenilin-1 (PS1) mice; *Methods*] and explored whether metaplastic mechanisms can augment plasticity and promote associativity (21). We noticed that L-LTP was impaired in this mouse model as early as 3–4 mo (before Aβ plaques are formed) and failed to show associative interactions such as STC. We further delineated the impaired molecular pathway associated with the lack of late plasticity and associativity. We noticed decreased expression of PKMζ, a critical PRP implicated in the establishment of long-term memory. In addition, the late phase of LTD (L-LTD) was not altered in APP/PS1 mice, but the positive associative interactions of LTP and LTD, a process called cross-capture, was compromised. Most importantly, metaplasticity via RyR priming in hippocampal synapses of APP/PS1 mice in vitro ameliorates the synaptic plasticity deficits in AD by reestablishing late plasticity and STC through activation of PKMζ. Thus, we propose that metaplastic mechanisms can be effectively used for the augmentiation of plasticity in the early stage of neurodegenerative diseases such as AD.

Significance

Under physiological conditions, metaplasticity is ideally suited to prepare neuronal networks for encoding specific information, thereby ensuring subsequent learning and long-lasting memory storage. Our memory capacity lies at the heart of all cognitive function, and the correct scaling of synaptic plasticity is vital for normal brain function. Here we present data from amyloid precursor protein (APP)/presenilin-1 (PS1) mice, a mouse model of Alzheimer's disease, indicating that the failure of neurons to scale the predisposition to undergo plasticity after earlier events (i.e., metaplasticity) might be a determinant for disease onset and progression. Our findings indicate that the induction of metaplasticity by ryanodine receptor activation contributes to the reestablishment of plasticity and associativity in hippocampal neurons of APP/PS1 mice and might be a potential therapeutic target.

NEUROSCIENCE

Statistics

The average values of the slope function of the field excitatory postsynaptic potential (fEPSP) per time point were analyzed by Wilcoxon signed-rank test (henceforth "Wilcoxon test") when compared within the group or the Mann–Whitney U test (henceforth "U test") when compared between groups. A t test (for the comparison between WT and APP/PS1 group) and one-way ANOVA with Dunnett's post hoc tests (for the comparison of the six groups) at the $P < 0.05$ significance level was used for the analysis of Western blot results. All experiments were performed blinded to the genotype of mice and/or blinded to the pharmacological treatment. Detailed descriptions of each experiments are provided in the *SI Methods*.

Results

RyR Priming Reestablishes Plasticity in APP/PS1 Mice. Previous studies have reported that LTP is impaired in the hippocampus of various AD mouse models (9, 22–24). Here we used a mouse model of AD that expresses a mutated chimeric mouse/human APP and the exon-9–deleted variant of human PS1, both linked to familial AD, under the control of a prion promoter element (APPswe/PS1dE9) (25). We set out to study L-LTP in these mice. After a stable baseline recording of 1 h in synaptic input S1 and S2 (Fig. 1A), strong tetanization (STET) was applied to S1, which resulted in a stable L-LTP lasting 240 min in WT mice (Fig. 1B, filled circles). Control stimulation of input S2 revealed stable potentials during the whole recording period (Fig. 1B, open circles). The same experimental design was used to test L-LTP in the hippocampal slices of APP/PS1 mice, which resulted only in early LTP (E-LTP; Fig. 1C, filled circles) without any alteration in the baseline recordings (Fig. 1C, open circles). Next, we examined the priming effect of RyR activation on the impaired L-LTP in APP/PS1 mice. After a 30-min stable baseline of S1 and S2, the RyR agonist RYA (10 μM) was bath-applied for 30 min and STET was applied to S1 30 min after the washout of RYA (thus, a total of 90 min baseline). Intriguingly, RYA priming significantly increased persistence of L-LTP without affecting its control input S2 (Fig. 1D). A comparison of levels of potentiation between WT, APP/PS1, and RyR-primed L-LTP in APP/PS1 at various time points is displayed in Fig. 1E.

RyR Priming Reestablishes STC in APP/PS1 Mice. Next, we probed whether the impaired L-LTP in APP/PS1 mice could still take part in STC. Two-pathway experiments of the "strong-before-weak" paradigm [STET in S1 followed by weak tetanization (WTET) in S2] were used for this investigation. First, we tested control STC in WT mice. Thus, STET was delivered to S1 to induce L-LTP, and, 30 min after the first STET, a WTET was applied to S2 to induce E-LTP. Here L-LTP was expressed in S2 lasting 4 h (Fig. 2A, filled and open circles), indicating expression of STC in WT mice. In the next series of experiments, we studied STC in APP/PS1 mice by using the same experimental paradigm as in Fig. 2A. Surprisingly, STC was not expressed in APP/PS1 mice, as the potentiation in S1 and S2 decayed to baseline levels within 2 h (Fig. 2B, filled and open circles). We tested whether priming stimulation of RyR could have any beneficial effects on STC in APP/PS1 mice. To test this hypothesis, STC was studied in the hippocampal slices of APP/PS1 mouse by using the same experimental design used in Fig. 2A or Fig. 2B, but RYA was bath-applied for 30 min and was washed out 30 min before the induction of L-LTP in S1. Intriguingly, S1 and S2 showed L-LTP lasting at least 4 h, thereby expressing STC (Fig. 2C, filled and open circles). A comparison of the potentiation levels at 240 min in S1 and S2 in WT (Fig. 2D, black bar), APP/PS1 (Fig. 2D, open bar) and RyR-primed APP/PS1 (Fig. 2D, gray bar) mice is displayed in Fig. 2D.
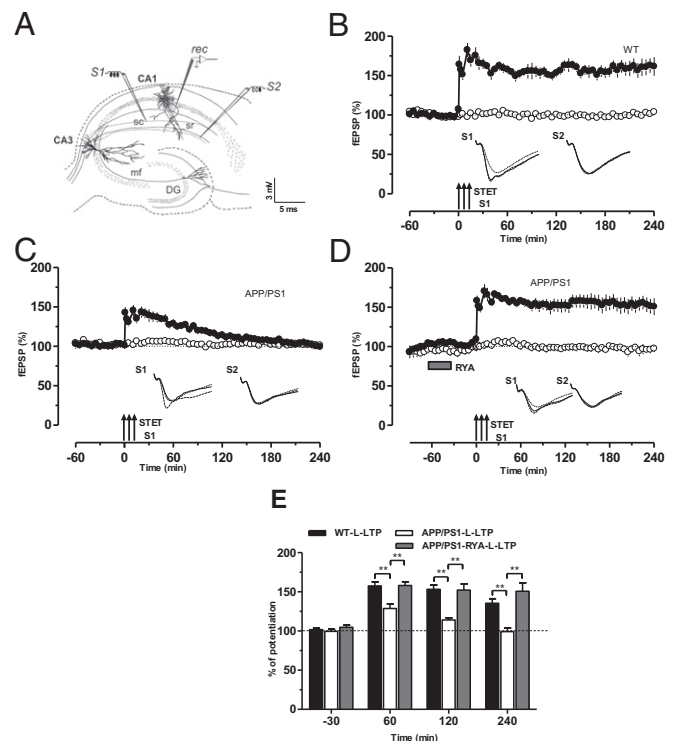

Fig. 1. RyR priming rescues the impaired L-LTP in APP/PS1 mice. (*A*) Schematic representation depicting the independent but convergent inputs onto pyramidal cells in the CA1 region of a hippocampal slice in vitro. The recording electrode (rec) placed in the stratum radiatum of CA1 records two independent fEPSPs elicited by the activation of two different inputs, S1 and S2, to the same neurons. DG, dentate gyrus; mf, mossy fiber; sc, Schaffer collaterals; sr, stratum radiatum. (*B*) A typical L-LTP induced by STET (arrows) in S1 (filled circles) in WT mice. Open circles represent a control stimulated synaptic input S2, which was stable for the whole recording period (*n* = 7). (*C*) Experimental design was the same as in *B*, but STET was applied to S1 to induce L-LTP in APP/PS1-derived slices, which resulted in LTP lasting less than 120 min (filled circles) without affecting the control input S2 (open circles; *n* = 7). (*D*) Priming of the hippocampal slices from APP/PS1 mice via bath application of RyR agonist RYA (gray rectangle; 10 μM) for 30 min and then washout for 30 min before the induction of LTP in S1 significantly increased the induction and persistence of L-LTP in S1 (filled circles). Control stimulation of S2 (open circles) revealed relatively stable potentials for the time course investigated (*n* = 8). (*E*) Bar graph represents the difference in the percentage of potentiation at −30 min, 60 min, 120 min, and 240 min after the induction of L-LTP between the three different conditions presented in *B–D*. Asterisks at 60, 120, and 240 min represent statistically significant potentiation (***P* < 0.01) with the compared group. Triplets of arrows represent STET applied for inducing L-LTP. Insets in each graph represent typical fEPSP traces recorded from synaptic inputs S1 and S2 at 30 min before (dotted line), 30 min after (broken line), and 4 h after (continuous line) induction of L-LTP. All data are plotted as mean ± SEM. Error bars indicate SEM. Calibration bar for all analog sweeps: 3 mV/5 ms.

RyR Priming Promotes Cross-Capture in APP/PS1 Mice. The protein synthesis-dependent late phase of LTP/LTD of one synaptic input has the capacity to transform the transient early LTD (E-LTD)/E-LTP in a second independent input into long-lasting L-LTD/L-LTP, a phenomenon referred to as cross-capture (26). We investigated whether cross-capture can be expressed in APP/PS1 mice. A prerequisite to be able to test this was to analyze L-LTD in APP/PS1 slices. In a control set of experiments, L-LTD in WT mice was induced by a strong low-frequency stimulation (SLFS) in S1, which resulted in an L-LTD lasting 240 min (Fig. 3A, filled circles) without altering the potentials of the control input S2 (Fig. 3A, open circles). Similarly, delivery of SLFS to the hippocampal slices of APP/PS1 mice resulted in a L-LTD lasting 240 min (Fig. 3B,
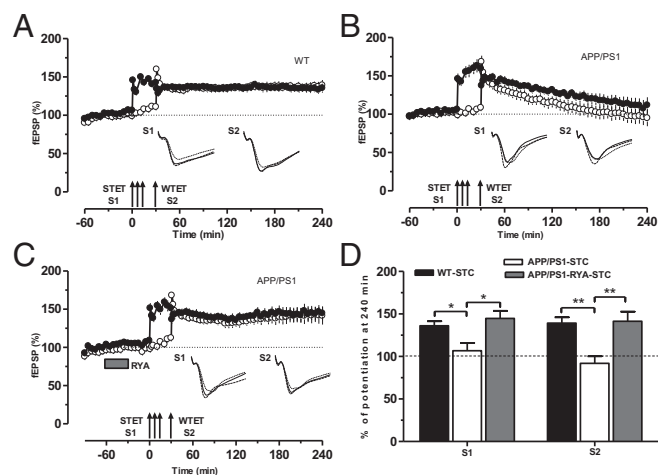
Fig. 2. RyR priming enables establishment of STC in APP/PS1 mice. (*A*) Control experiments showing STC induced by a strong-before-weak protocol in WT mice. Induction of L-LTP by STET in S1 (filled circles) was followed by E-LTP induced by WTET (single arrow) in S2 (open circles). Here E-LTP was transformed into an L-LTP, showing STC (*n* = 7). (*B*) Experimental design was similar to *A*, but STC was induced in APP/PS1 mice and potentiation of both synaptic inputs S1 (filled circles) and S2 (open circles) returned to baseline levels within 180 min, showing impaired STC (*n* = 8). (*C*) As in *B*, except that RYA (10 μM) was bath-applied for 30 min and then washed out for 30 min. Here L-LTP in S1 was rescued (filled circles) and E-LTP in S2 was transformed into L-LTP in S2 (open circles), expressing STC (*n* = 7). (*D*) Bar graph showing differences in the level of potentiation of synaptic input S1 and S2 after the induction of L-LTP or E-LTP, respectively, at 240 min between the three different conditions presented in *A*–*C*. Asterisks indicate significant group differences in potentiation (*P < 0.05 and **P < 0.01). Symbols/traces are as in Fig. 1.

filled circles). To study cross-capture in WT mice, a stable baseline was recorded for 1 h, SLFS was delivered to S1 to induce L-LTD, and a WTET was delivered to S2 at 45 min to induce E-LTP. Here, E-LTP in S2 was transformed to L-LTP (Fig. 3*C*, filled and open circles), expressing cross-capture. The same cross-capture paradigm was then applied to hippocampal slices of APP/PS1 mice. Surprisingly, E-LTP in S2 was not transformed to L-LTP, whereas L-LTD maintenance was normal as in Fig. 3*A* (Fig. 3*D*, filled and open circles), indicating the failure of cross-capture establishment in the CA1 pyramidal neurons of APP/PS1 mice. We have reported earlier that metaplastic priming of RyR results in the activation of PKMζ and promotion of STC (17). Thus, we hypothesized that metaplastic activation of RyR could also rescue cross-capture in APP/PS1 mice. To test this possibility, the same cross-capture paradigm was used as in Fig. 3*C* or Fig. 3*D*, except that RYA (10 μM) was bath-applied for 30 min and washed out 30 min before the induction of L-LTD in S1. In this experimental condition, E-LTP in S2 was transformed into L-LTP, resulting in cross-capture (Fig. 3*E*). A comparison of the depression and potentiation levels at 240 min in S1 and S2 in WT (Fig. 3*F*, black bar), APP/PS1 (Fig. 3*F*, open bar), and RyR-primed APP/PS1 (Fig. 3*F*, gray bar) mice is displayed in Fig. 3*F*.

RyR Priming Triggers New Synthesis of PRPs. It was proposed earlier that prior activation of group I metabotropic glutamate receptors (mGluRs) or RyRs facilitates the subsequent LTP through local synthesis of PRPs (17, 18, 27). To elucidate whether this also happens in APP/PS1 mice, the protein synthesis inhibitor anisomycin (ANI; 25 μM) was coapplied during RYA priming. As predicted, protein synthesis inhibition did not affect the initial induction of LTP but caused it to decay rapidly to the baseline levels within 2 h after STET (Fig. 4*A*, filled circles). Thus, new PRPs are being synthesized during RYA priming and are

instrumental to the rescue of LTP in APP/PS1 mice. Next, we probed whether inhibition of protein synthesis during RYA priming prevents STC in APP/PS1 mice. As shown in Fig. 4*B*, application of ANI during RYR priming prevented STC in APP/PS1 mice.

Next, we addressed the question of which PRPs are being synthesized during RyR priming in APP/PS1 mice. We have reported earlier that group 1 mGluR or RyR activation leads to the new synthesis of PKMζ in rat hippocampal slices (17, 27). In this study, we estimated and compared the total PKMζ level in the hippocampal CA1 region of WT and APP/PS1 mice. As shown in Fig. 4 *C* and *D*, we observed a statistically significant decrease in the level of total PKMζ in APP/PS1 mice compared with WT mice. Motivated by these findings, we investigated whether RYA priming in APP/PS1 mice also occur through local synthesis of PKMζ. To test this, the atypical PKC inhibitor myr-zeta inhibitory peptide (ZIP; 1 μM) was initially applied for 15 min before RYA was coapplied for 30 min along with ZIP. Under these conditions, we induced L-LTP in S1 30 min after the washout of the drug. Indeed, the effect of RyR priming on L-LTP in APP/PS1 was completely abolished by myr-ZIP (Fig. 4*E*, filled circles). Control experiments using an inactive scrambled peptide of myr-ZIP, scr-ZIP (1 μM), showed no
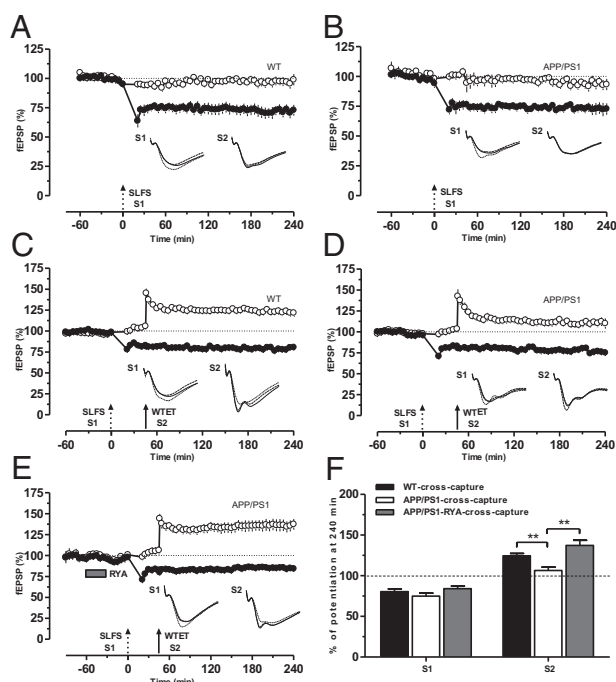

Fig. 3. RyR priming promotes cross-capture in APP/PS1 mice. (*A*) In WT mice, an SLFS (broken arrow) applied to S1 resulted in a significant L-LTD (filled circles) lasting for 4 h. Control input S2 (open circles) that received test pulses was stable during the whole recording period (*n* = 11). (*B*) The same as *A*, except that L-LTD was induced in APP/PS1 mice (*n* = 8). (*C*) In WT mice, E-LTP by a WTET (single arrow) in S2 (open circles) can be converted to L-LTP provided L-LTD induced by SLFS in S1was induced by SLFS in S1 (filled circles) 45 min before the induction of E-LTP, showing cross-capture (*n* = 7). (*D*) Experimental design similar to *C*, with the exception that cross-capture was studied in APP/PS1 mice. Here E-LTP was not transformed into L-LTP in S2 (open circles), showing no cross-capture (*n* = 7). (*E*) Priming stimulation with RYA (10 μM) for 30 min enabled the establishment of cross-capture in APP/PS1 mice, as E-LTP in S2 was transformed into L-LTP (open circles; *n* = 9). (*F*) Bar graph showing differences in the levels of potentiation of synaptic input S2 after the WTET at 240 min between the three different conditions presented in *C*–*E*, whereas the depression of synaptic input S1 after the SLFS at 240 min was not altered. Asterisks indicate significant group differences in potentiation (**P < 0.01). Single arrow represents the time point of induction of E-LTP by WTET.
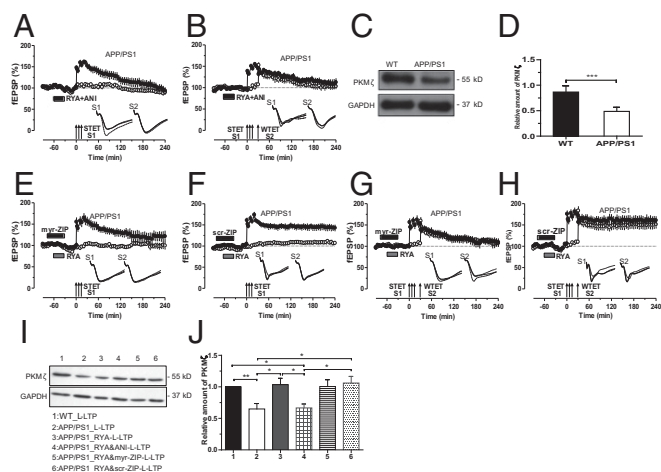
NEUROSCIENCE

Fig. 4. RyR priming triggers new synthesis of PKMζ in APP/PS1 mice. (*A*) Application of the protein synthesis inhibitor ANI (25 μM) during RYA priming abolished the priming effect of RYA in APP/PS1 mice, leading to a decayed LTP (filled circles) without affecting the baseline potentials in S2 (open circles; *n* = 8). (*B*) Similarly, when ANI (25 μM) was coapplied with RYA for 30 min, no STC was observed in APP/PS1 mice, as input S1 and S2 showed only E-LTP (*n* = 7). (*C*) Western blot and quantification (*D*) of PKMζ protein reduction in APP/PS1 mice normalized to GAPDH (***P* < 0.001). The Western blots were repeated three times, and, in each group, 12 slices were used for tissue collection. (*E*) Administration of PKMζ inhibitor myr-ZIP (1 μM) alone for 15 min and then together with RYA for 30 min attenuated the rescued L-LTP in S1 (filled circles) in APP/PS1 mice, whereas the potentials of the control pathway S2 (open circles) remained stable throughout the entire recording period (*n* = 7). (*F*) The inactive scrambled version of myr-ZIP, scr-ZIP (1 μM), was bath-applied alone for 15 min and then together with RYA for 30 min, showing no effects on RYA-primed L-LTP in APP/PS1 mice (*n* = 6). (*G*) PKMζ blockade by myr-ZIP (1 μM) 15 min before and during RYA priming prevented not only the maintenance of L-LTP in S1 (filled circles) but also the transformation of E-LTP into L-LTP in S2 (open circles) in APP/PS1 mice, expressing no STC (*n* = 7). (*H*) Application of scr-ZIP 15 min before and during RYA priming had no effect on the primed STC in APP/PS1 mice (*n* = 6). (*I*) Western blot and quantification (*J*) of PKMζ protein expression revealed a higher expression of PKMζ in APP/PS1 mice 1 h after the induction of RYA-primed L-LTP (group 3) in comparison with nonprimed L-LTP group (group 2) and RYA-primed L-LTP in the presence of the ANI group (group 4). Although the application of myr-ZIP together with RYR priming and L-LTP inhibited PKMζ function as seen in Fig. 4 *E* and *G*, it had no significant effect on the expression rate of PKMζ (group 5). Application of control peptide, scr-ZIP, had no effect on the expression level of PKMζ (group 6). In addition, PKMζ level after L-LTP induction in APP/PS1 mice (group 2) is significantly lower than that in WT mice (group 1). The values of the individual groups were calculated in relation to the control group with GAPDH as a loading control (**P* < 0.05 and ***P* < 0.01). Western blot analyses were repeated six times, and, in each group, 14–19 slices were used for tissue collection. Symbols/traces are as in Fig. 1.

inhibitory effect on the primed L-LTP in APP/PS1 mice (Fig. 4*F*). In both cases, the control input S2 showed stable potentials during the whole recording session.

Having found that priming by RyR activation results in the generation of PKMζ, possibly normalizing the availability of this kinase in APP/PS1 mice, we next probed whether the newly generated PKMζ is also mandatory for the establishment of STC in APP/PS1 mice. Bath administration of myr-ZIP alone for 15 min and together with RYA similar to Fig. 4*E* prevented not only the primed L-LTP in S1 but also the transformation of E-LTP into L-LTP in S2 (Fig. 4*G*, filled and open circles). Thus, PKMζ plays an important role during the RyR-primed STC in APP/PS1 mice. Control experiments with scr-ZIP showed unaltered RYA-primed STC (Fig. 4*H*). To further confirm our pharmacological findings, biochemical experiments were conducted to confirm the expression level of PKMζ in APP/PS1 mice and during priming stimulation by

RyR. As shown in Fig. 4 *I* and *J*, compared with WT mice, PKMζ expression level after L-LTP induction was significantly decreased in the hippocampal CA1 region of APP/PS1 mice. Strikingly, in APP/PS1 mice, PKMζ level was increased 1 h after RYA-primed L-LTP (group 3) in comparison with the L-LTP group without RYA priming (group 2) and RYA-primed L-LTP in the presence of ANI (group 4). The application of myr-ZIP together with RYA during priming inhibited PKMζ function, as shown in Fig. 4 *E* and *G*, but it had no effect on the expression rate of PKMζ (group 5; no statistically significant decrease in the expression of PKMζ compared with group 3; Fig. 4*I*), similar to previous reports (17, 27). The control peptide scr-ZIP had no effect on the function of PKMζ as shown in Fig. 4 *F* and *H*, and the expression of PKMζ (group 6; Fig. 4*I*).

These data reveal that PKMζ expression is decreased in the hippocampal CA1 region of APP/PS1 mice under basal conditions and also during activity-dependent plasticity and that RyR-mediated metaplasticity up-regulates the synthesis of PKMζ.

PKMζ Maintains STC and Cross-Capture in APP/PS1 Mice. In conventional STC, PKMζ is identified as the first LTP-specific PRP (17, 27, 28). To test whether a similar mechanism was also present during RyR-mediated metaplasticity in APP/PS1 mice, myr-ZIP was bath-applied 60 min after the induction of RYA-primed L-LTP until the end of the experiment. As shown in Fig. 5*A* (filled circle), primed L-LTP slowly decayed to baseline level. In contrast, control experiments using scr-ZIP showed normal maintenance of primed LTP (Fig. 5*B*). In both cases, the control input S2 showed stable potentials during the entire recording period.

Similarly, the effect of PKMζ inhibition on RYA-primed STC was investigated. Bath application of myr-ZIP 30 min after the establishment of RYA-primed STC prevented L-LTP maintenance in S1 and S2 (Fig. 5*C*, open and filled circles), thus expressing no STC. Control experiments with scr-ZIP showed normal primed STC (Fig. 5*D*). Not only in STC but also in cross-capture, PKMζ is captured by weakly tetanized synapses (28); therefore, the next question we probed was whether PKMζ is also a PRP in RYA-primed cross-capture. Bath application of myr-ZIP 75 min after the establishment of RYA-primed cross-capture prevented only the transformation of E-LTP into L-LTP in S1 (Fig. 5*E*, open circles), but had no effects on L-LTD in S2 (Fig. 5*E*, filled circles).

Recent studies have shown that ZIP used for inhibiting PKMζ may also inhibit other atypical PKC isotypes such as PKCi/λ (29), and also that ZIP could alter neuronal and network activity in a way that might be independent of PKMζ (30, 31). In addition, PKCi/λ can compensate PKMζ in certain conditions (29, 32, 33). We have ruled out the possibility of the latter by checking the PKCi/λ level in control and APP/PS1 mice. Our Western blot analysis shows no difference in the level of PKCi/λ between control and APP/PS1 mice (Fig. S1 *A and B*). RyR-mediated rescue of plasticity and associativity is specifically mediated by PKMζ because PKMζ antisense oligonucleotide (20 μM) prevents RyR-primed L-LTP and STC (Fig. S2 *A–D*).

Discussion

Metaplasticity, a fundamental property of synapses in the brain, is capable of tuning the synapses and networks for neural plasticity (15). Our findings provide important insight into metaplasticity mechanisms, showing that RyR activation in the hippocampal circuitry of the AD mouse model of APP/PS1 mice prevents impairments of synaptic plasticity, including L-LTP, STC, and cross-capture. How does RyR priming prevent synaptic plasticity deficits in AD? Our study indicates that, in APP/PS1 mice, the metaplasticity properties of synaptic populations are lost which shifts the BCM (Bienenstock, Cooper, and Munro) (34) curve toward the right—that is, a higher threshold
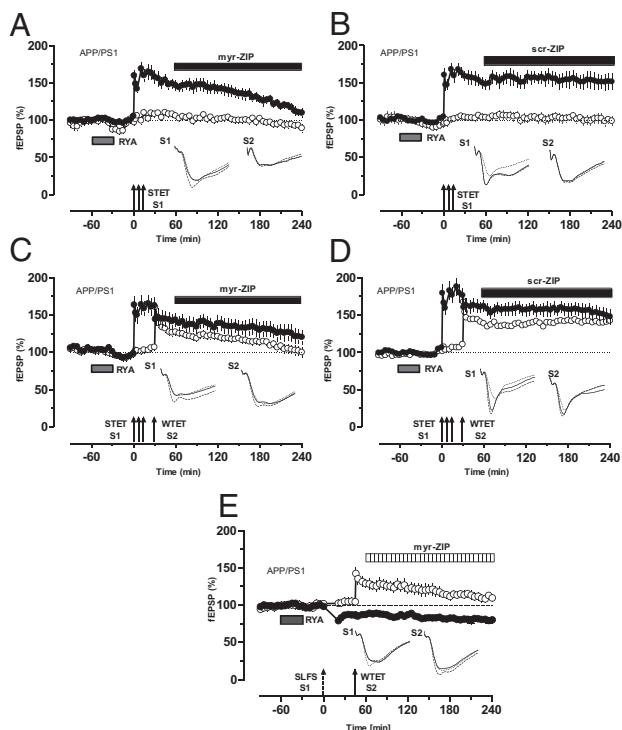
Li et al.

Fig. 5. Identity of PRP in primed L-LTP in APP/PS1 mice. (*A*) Application of the PKMζ inhibitor myr-ZIP (1 μM) 60 min after induction of L-LTP prevented RYA-primed L-LTP (filled circles). Baseline potentials recorded from S2 (open circles) showed stable potentials during the entire recording period (*n* = 7). (*B*) Application of scr-ZIP (1 μM) starting 60 min after induction of L-LTP until the end of recording had no effect on the maintenance of RYA-primed L-LTP in APP/PS1 mice (*n* = 7). (*C*) Continuous blockade of PKMζ by myr-ZIP (1 μM) 30 min after the establishment of STC prevented RYA-primed STC, as S1 and S2 decayed to baseline gradually (*n* = 7). (*D*) Application of scr-ZIP starting 30 min after the establishment of STC until the end of the experiment had no effect on RYA-primed STC in APP/PS1 mice (*n* = 7). (*E*) Blockade of PKMζ by myr-ZIP starting 75 min after the establishment of cross-capture had no effect on the L-LTD in S1 (filled circles) but prevented the conversion of E-LTP to L-LTP in S2 (open circles; *n* = 7). Symbols/traces are as in Fig. 1.

for inducing plasticity (35). RyR priming rescues it by increasing calcium level, thereby lowering the threshold for inducing plasticity and bringing L-LTP back to the positive part of the BCM curve.

It can be argued that the activation of RyR would worsen the AD neuronal network by virtue of the classic calcium hypothesis (36, 37), but we rather obtained a rescue effect. It has been reported earlier that 3–4-mo-old APP/PS1 mice do not have resting calcium levels that are different from those of WT mice (38). Indeed, our basal calcium level analysis supports this finding and provides additional evidence that the levels of calcium during metaplastic stimulation by RYA is also unaltered between WT and APP/PS1 mice (difference between control and 10 μM RYA application, $P > 0.1$, *t* test). These mice at this age do not show Aβ plaques, raising a question about the status of calcium overload, which is usually associated with Aβ plaques (38). As the animal model used in this study is of age 3–4 mo, it can be assumed that acute effects of elevated calcium by RyR-dependent metaplasticity might have resulted in plasticity compensation. However, we do not rule out the possibility that, in aged APP/PS1 mice (≥6 mo), elevated resting calcium levels and Aβ plaque may have the opposite effect, i.e., acceleration of neurodegeneration as a result of increased calcium level by RyR-dependent metaplasticity.

The lack of STC observed in the APP/PS1 mice could be the result of two reasons: (*i*) inability of the synaptic population to

create a synaptic tag and (*ii*) inability of the strongly tetanized input to generate enough PRPs to initiate STC. We rule out the first possibility because RyR priming before the induction of L-LTP indeed transforms the E-LTP in the second synaptic input to L-LTP, providing electrophysiological evidence that a synaptic tag is present. Indeed, our second assumption is supported by pharmacological and biochemical evidence. Inhibition of protein synthesis or PKMζ prevents the RyR priming effect and associated enhancement of plasticity and associativity. The biochemical evidence is also in this line, as PKMζ expression level is decreased in the hippocampal CA1 region of APP/PS1 mice and RyR priming increases its expression. As PKMζ is essential for the consolidation of LTP and STC (28), the decreased amount of PKMζ could explain why LTP and STC are impaired in APP/PS1 mice. The persistence of L-LTD in APP/PS1 mice is not altered, which suggests that not all forms of plasticity are compromised in these mice. This observation is in agreement with earlier findings that application of Aβ has no effect on hippocampal LTD (10–12). We have reported earlier that L-LTD can be maintained during PKMζ inhibition, as depressed synapses rely more on brain-derived neurotrophic factor (27, 28). The absence of cross-capture in APP/PS1 mice is most likely a result of the lack of PRPs such as PKMζ as RyR priming and subsequent induction of L-LTD was able to reinstate cross-capture.

Autopsy brain tissue samples derived from patients with neuropathologically confirmed AD showed that PKMζ aggregates with neurofibrillary tangles in their limbic or medial temporal lobe structures, such as hippocampal formation, entorhinal cortex, and amygdala, which may inhibit the normal activity of this kinase in modulating the trafficking of AMPA receptors at synapses (39). In addition, subcellular distribution of GluA2 receptors and PKMζ is altered in the aging brain, showing a decreased density of synaptic GluA2 receptors in large dendritic spines coexpressing PKMζ, and this decrease correlates with impaired recognition memory (40). The present data show that RyR priming reverses synaptic dysfunction in APP/PS1 mice through metaplastic up-regulation of PKMζ. Recently, the specificity of ZIP for inhibiting the effects of PKMζ on L-LTP and long-term memory has been brought into question (29, 32, 41). In the present study, we specifically prevented PKMζ activity by using PKMζ antisense molecules similar to that in a previous report (33), confirming that the RyR priming-induced PRP is PKMζ and not any other atypical PKCs. A recent study has suggested that PKCι/λ can compensate for the lack of PKMζ in KO mice (33). It can be argued that reduced level of PKMζ in AD mice may not be important for synaptic plasticity deficits, particularly if PKCι/λ is upregualted. This possibility is excluded in APP/PS1 mice, as the level of PKCι/λ is similar to that of control animals, and, in addition, L-LTP and STC were still not present in APP/PS1 mice.

Theoretical models of dynamically learning neural networks predict that ongoing memory storage relies on synapses that exhibit multiple states with different levels of plasticity over a wide range of time scales, linked by metaplastic transitions (42). Our study provides compelling evidence that, even in AD, the activated neural network is capable of incorporating metaplastic states, thereby compensating dysregulated synaptic plasticity in the hippocampal memory circuitry. Our findings are in agreement with recent observation by Megill et al. in which the authors proposed that the synaptic defect occurring in AD mouse models may result from the inability of the synaptic populations to undergo metaplasticity, especially during developmental stages (35). We propose that enabling a synaptic population for metaplasticity can reestablish plasticity and associative plasticity in AD mouse models. In the future, it would be intriguing to explore whether such a metaplasticity form can ameliorate the learning and memory deficits of AD in behaving mice.

NEUROSCIENCE

Methods

All procedures concerning animals were approved by the animal welfare representative of Technische Universität Braunschweig and the Landesamt für Verbraucherschutz und Lebensmittelsicherheit [Oldenburg, Germany; Az. §4 (02.05) TSchB TU BS] and National University of Singapore. Animals were kept under standard housing conditions with a 12-h dark/ light cycle. More details about slice preparation, incubation, electrophysiology procedures, and pharmacology are provided in the *SI Methods*.

1. Bäckman L, Small BJ, Fratiglioni L (2001) Stability of the preclinical episodic memory deficit in Alzheimer's disease. *Brain* 124:96–102.
2. McLean CA, et al. (1999) Soluble pool of Abeta amyloid as a determinant of severity of neurodegeneration in Alzheimer's disease. *Ann Neurol* 46:860–866.
3. Selkoe DJ (2001) Alzheimer's disease results from the cerebral accumulation and cytotoxicity of amyloid beta-protein. *J Alzheimers Dis* 3:75–80.
4. Walsh DM, et al. (2002) Naturally secreted oligomers of amyloid β protein potently inhibit hippocampal long-term potentiation in vivo. *Nature* 416:535–539.
5. Shankar GM, et al. (2008) Amyloid-beta protein dimers isolated directly from Alzheimer's brains impair synaptic plasticity and memory. *Nat Med* 14:837–842.
6. Walsh DM, Selkoe DJ (2004) Deciphering the molecular basis of memory failure in Alzheimer's disease. *Neuron* 44:181–193.
7. Selkoe DJ (2002) Alzheimer's disease is a synaptic failure. *Science* 298:789–791.
8. Haass C, Selkoe DJ (2007) Soluble protein oligomers in neurodegeneration: Lessons from the Alzheimer's amyloid β-peptide. *Nat Rev Mol Cell Biol* 8:101–112.
9. Gong B, et al. (2004) Persistent improvement in synaptic and cognitive functions in an Alzheimer mouse model after rolipram treatment. *J Clin Invest* 114:1624–1634.
10. Li S, et al. (2009) Soluble oligomers of amyloid Beta protein facilitate hippocampal long-term depression by disrupting neuronal glutamate uptake. *Neuron* 62:788–801.
11. Raymond CR, Ireland DR, Abraham WC (2003) NMDA receptor regulation by amyloid-beta does not account for its inhibition of LTP in rat hippocampus. *Brain Res* 968:263–272.
12. Wang HW, et al. (2002) Soluble oligomers of beta amyloid (1-42) inhibit long-term potentiation but not long-term depression in rat dentate gyrus. *Brain Res* 924:133–140.
13. Adasme T, et al. (2011) Involvement of ryanodine receptors in neurotrophin-induced hippocampal synaptic plasticity and spatial memory formation. *Proc Natl Acad Sci USA* 108:3029–3034.
14. Rönicke R, et al. (2011) Early neuronal dysfunction by amyloid β oligomers depends on activation of NR2B-containing NMDA receptors. *Neurobiol Aging* 32:2219–2228.
15. Abraham WC (2008) Metaplasticity: Tuning synapses and networks for plasticity. *Nat Rev Neurosci* 9:387.
16. Hulme SR, Jones OD, Abraham WC (2013) Emerging roles of metaplasticity in behaviour and disease. *Trends Neurosci* 36:353–362.
17. Li Q, et al. (2014) Making synapses strong: Metaplasticity prolongs associativity of long-term memory by switching synaptic tag mechanisms. *Cereb Cortex* 24:353–363.
18. Mellentin C, Jahnsen H, Abraham WC (2007) Priming of long-term potentiation mediated by ryanodine receptor activation in rat hippocampal slices. *Neuropharmacology* 52:118–125.
19. Redondo RL, Morris RG (2011) Making memories last: The synaptic tagging and capture hypothesis. *Nat Rev Neurosci* 12:17–30.
20. Frey U, Morris RG (1998) Synaptic tagging: Implications for late maintenance of hippocampal long-term potentiation. *Trends Neurosci* 21:181–188.
21. Holcomb L, et al. (1998) Accelerated Alzheimer-type phenotype in transgenic mice carrying both mutant amyloid precursor protein and presenilin 1 transgenes. *Nat Med* 4:97–100.
22. Trinchese F, et al. (2004) Progressive age-related development of Alzheimer-like pathology in APP/PS1 mice. *Ann Neurol* 55:801–814.

23. Ma T, et al. (2010) Dysregulation of the mTOR pathway mediates impairment of synaptic plasticity in a mouse model of Alzheimer's disease. *PLoS One* 5:e12845.
24. Chapman PF, et al. (1999) Impaired synaptic plasticity and learning in aged amyloid precursor protein transgenic mice. *Nat Neurosci* 2:271–276.
25. Borchelt DR, et al. (1997) Accelerated amyloid deposition in the brains of transgenic mice coexpressing mutant presenilin 1 and amyloid precursor proteins. *Neuron* 19:939–945.
26. Sajikumar S, Frey JU (2004) Late-associativity, synaptic tagging, and the role of dopamine during LTP and LTD. *Neurobiol Learn Mem* 82:12–25.
27. Sajikumar S, Korte M (2011) Metaplasticity governs compartmentalization of synaptic tagging and capture through brain-derived neurotrophic factor (BDNF) and protein kinase Mzeta (PKMzeta). *Proc Natl Acad Sci USA* 108:2551–2556.
28. Sajikumar S, Navakkode S, Sacktor TC, Frey JU (2005) Synaptic tagging and cross-tagging: The role of protein kinase Mzeta in maintaining long-term potentiation but not long-term depression. *J Neurosci* 25:5750–5756.
29. Volk LJ, Bachman JL, Johnson R, Yu Y, Huganir RL (2013) PKM-ζ is not required for hippocampal synaptic plasticity, learning and memory. *Nature* 493:420–423.
30. LeBlancq MJ, McKinney TL, Dickson CT (2016) ZIP it: Neural silencing is an additional effect of the PKM-Zeta inhibitor zeta-inhibitory peptide. *J Neurosci* 36:6193–6198.
31. Sadeh N, Verbitsky S, Dudai Y, Sega IM (2015) Zeta Inhibitory Peptide, a candidate inhibitor of Protein Kinase Mζ, is excitotoxic to cultured hippocampal neurons. *J Neurosci* 35:12404–12411.
32. Lee AM, et al. (2013) Prkcz null mice show normal learning and memory. *Nature* 493:416–419.
33. Tsokas P, et al. (2016) Compensation for PKMζ in long-term potentiation and spatial long-term memory in mutant mice. *eLife* 5:5.
34. Bienenstock EL, Cooper LN, Munro PW (1982) Theory for the development of neuron selectivity: Orientation specificity and binocular interaction in visual cortex. *J Neurosci* 2:32–48.
35. Megill A, et al. (2015) Defective age-dependent metaplasticity in a mouse model of Alzheimer's disease. *J Neurosci* 35:11346–11357.
36. Chami M, Checler F (2014) Ryanodine receptors: Dual contribution to Alzheimer disease? *Channels (Austin)* 8:168.
37. LaFerla FM (2002) Calcium dyshomeostasis and intracellular signalling in Alzheimer's disease. *Nat Rev Neurosci* 3:862–872.
38. Kuchibhotla KV, et al. (2008) Abeta plaques lead to aberrant regulation of calcium homeostasis in vivo resulting in structural and functional disruption of neuronal networks. *Neuron* 59:214–225.
39. Crary JF, Shao CY, Mirra SS, Hernandez AI, Sacktor TC (2006) Atypical protein kinase C in neurodegenerative disease I: PKMzeta aggregates with limbic neurofibrillary tangles and AMPA receptors in Alzheimer disease. *J Neuropathol Exp Neurol* 65:319–326.
40. Hara Y, et al. (2012) Synaptic distributions of GluA2 and PKMζ in the monkey dentate gyrus and their relationships with aging and memory. *J Neurosci* 32:7336–7344.
41. Ren SQ, et al. (2013) PKCλ is critical in AMPA receptor phosphorylation and synaptic incorporation during LTP. *EMBO J* 32:1365–1380.
42. Fusi S, Drew PJ, Abbott LF (2005) Cascade models of synaptically stored memories. *Neuron* 45:599–611.